

# The Effect of Heart Rate and Atrial Contraction on Left Ventricular Function

Rosie K Barrows<sup>1</sup>, Marina Strocchi<sup>1</sup>, Christoph M Augustin<sup>2</sup>, Matthias A F Gsell<sup>2</sup>, Caroline H Roney<sup>3</sup>, Jose A Solis-Lemus<sup>1</sup>, Hao Xu<sup>1</sup>, Karli K Gillette<sup>2</sup>, Ronak Rajani<sup>1</sup>, John Whitaker<sup>1</sup>, Edward J Vigmond<sup>4</sup>, Martin J Bishop<sup>1</sup>, Gernot Plank<sup>2</sup>, Steven A Niederer<sup>1</sup>

<sup>1</sup> King's College London, London, United Kingdom

<sup>2</sup> Medical University of Graz, Graz, Austria

<sup>3</sup> Queen Mary University of London, London, United Kingdom

<sup>4</sup> IHU Liryc, Bordeaux, France

## Abstract

*Heart rate (HR) and effective atrial contraction affect left ventricular (LV) output. This is particularly relevant in atrial fibrillation (AF) patients, where HR is fast and irregular and atrial contraction almost completely absent. The effect of AF on the LV remains understudied, although a better understanding of these mechanisms could improve AF patient care. We have used a four-chamber electromechanics model to quantify how AF impacts LV function. Our model accounts for the effect of the pericardium and the coupling with the circulatory system, represented as a closed loop, providing physiological preload and afterload for the heart. The heart model was used for a factorial study with two HRs (70 bpm and 120 bpm) and in the presence and in the absence of atrial contraction. We found that an increased HR and lack of atrial contraction alone led to a small decrease in ejection fraction (42% to 40% and 42% to 41%, respectively). However, the interaction between an increased HR and lack of atrial contraction led to a drop in ejection fraction from 42% to 36%. This study demonstrates that our four-chamber heart models can be used to investigate the effect of rapid HR and ineffective atrial contraction on LV output and that AF can significantly impact LV function. This motivates further studies investigating the effect of AF on the whole heart.*

## 1. Introduction

Atrial fibrillation (AF) is the most common cardiac arrhythmia with a worldwide prevalence estimated to exceed 45 million [1]. During AF, re-entrant waves in the atria interfere with normal heart rhythm, leading to a rapid, irregular heart rate (HR) and almost complete absence of atrial contraction [2]. The associated increased risk of blood clots and stroke means a more complete understanding of the disease is vital. However, the interaction between the

atria and ventricles is complex and still not fully understood. This makes investigations of the effect of AF on ventricular output challenging.

The atria modulate ventricular filling in three different ways: acting as a reservoir during systole, a conduit phase during diastole, and a phase of active contraction during late diastole [2]. This final phase is of particular relevance in patients with AF, as the ineffective contraction of the atria leads to sub-optimal loading of the ventricles. Clinical research has shown that the loss of atrial contraction associated with AF decreases cardiac output by approximately 15-20% [2].

One approach to investigating the interaction of the atria and ventricles is through the use of computational models for cardiac electromechanics. Early models focused on only one or two cardiac chambers. However, significant progress has recently been made towards four-chamber models which include the major blood vessels and account for the effect of the pericardium [3], [4]. These more realistic models allow for the simulation of physiological motion and can be used to investigate atrioventricular interaction. In this study, we used a four-chamber electromechanics model to study how increased HR and absent atrial contraction alter left ventricular (LV) function.

## 2. Methods

The four-chamber heart geometry used in this study was generated from ECG-gated CT of a 78 year old male with AF. Whole heart images (in-plane resolution: 0.39 mm, slice thickness: 0.6 mm) were acquired throughout the cardiac cycle and a segmentation of the end-diastolic image was used to generate a mesh with linear tetrahedra.

Ventricular and atrial myofibre orientations were assigned to the mesh, using the Laplace-Dirichlet rule-based method by Bayer et al [5]. The intersection between the mitral valve plane, tricuspid valve plane and the ventricles

was used to define the base and the point on the LV epicardium furthest from the left atrium (LA) was chosen as the apex. To compute the myofibre orientations, the epicardium of the ventricles and the endocardial surfaces of the LV and right ventricle (RV) were extracted from the mesh and used to define different Laplace solutions. Endocardial/epicardial fibre and sheet angles were defined as  $-60^\circ/+60^\circ$  and  $-65^\circ/+25^\circ$ , respectively. For the atrial fibres, universal atrial coordinates [6] were used to map myofibre orientations from a human ex-vivo DTMRI dataset. An epicardial and endocardial layer of fibres were then assigned based on a transmural Laplace solution.

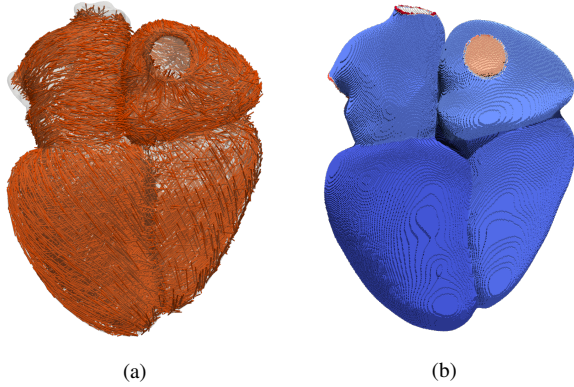


Figure 1: (a) Myofibre directions assigned to the atria and ventricles. (b) Segmentation of the CT images after post-processing and smoothing.

## 2.1. Electromechanics simulation

A reaction-eikonal model [7] was used to simulate the electrical activation of the heart, leading to a solution for activation time  $t_a(\mathbf{x})$  as a function of node location. Atrioventricular conduction pathways were not explicitly modelled in the simulations. Instead, a 1 element thick passive layer was defined between the atria and ventricles to prevent unphysiological activation and to fully control atrioventricular delay. Atrial activation was initiated at a point behind the superior vena cava, to approximate the sinoatrial node. The ventricles were then stimulated at the apex with a delay of 100 ms.

Atrial and ventricular myocardium were simulated as transversely isotropic conduction media, with preferred conduction direction aligned with local myofibre orientation. Two additional regions were also defined: one to represent the Bachmann's bundle in the atria and the other to simulate fast endocardial activation in the ventricular endocardium.

In the mechanics model, the atria and ventricles were modelled as a transversely isotropic, hyperelastic and nearly incompressible material with the Guccione law [9].

Table 1: Parameters for conduction velocity in the fibre ( $CV_f$ ) and transverse ( $CV_t$ ) direction used in the four active regions of the heart model [8].

Region	$CV_f$ (m/s)	$CV_t$ (m/s)
Atria	0.90	0.36
Bachmann's bundle	3.2	1.3
Ventricles	0.60	0.24
FEC	3.0	1.2

The material parameters for atria and ventricles were set based on [3]. The parameters for the ventricles were then adjusted to achieve a physiological LV ejection fraction (EF) above 40%. The parameters set for the atria and ventricles respectively were as follows:  $a = 3.0$ ,  $b_f = 25.0$ ,  $b_{fs} = 11.0$ ,  $b_t = 9.0$  and  $a = 2.2$ ,  $b_f = 15.0$ ,  $b_{fs} = 11.0$ ,  $b_t = 9.0$ , in range with values estimated in [10]. This accounts for the atria containing significantly higher collagen concentrations than the LV [11]. All other tissues (aortic wall, pulmonary artery and valve planes) were modelled as neo-Hookean and material parameters set according to previous studies [4] [3]. Incompressibility was enforced for all tissue types using a penalty method, with a bulk modulus  $k = 1000.0$  kPa.

A phenomenological active tension model [12] was used to handle active tension in the atria and ventricles, with active tension rise triggered by nodal activation time ( $t_a(\mathbf{x})$ ) as:

$$S_a(\mathbf{x}, t) = T_{peak} \phi(\lambda) \tanh^2\left(\frac{t_s}{\tau_r}\right) \tanh^2\left(\frac{t_{dur} - t_s}{\tau_d}\right), \quad 0 < t_s < t_{dur}$$

$$\phi(\lambda) = \tan(l d(\lambda - \lambda_0)), \quad t_s = t - t_a(\mathbf{x}) - t_{emd}$$

for  $t_s = t - t_a(\mathbf{x}) - t_{emd}$ , where  $T_{peak}$  is the peak in active tension and  $t$ ,  $t_{emd}$ ,  $\tau_r$ ,  $\tau_d$  and  $t_{dur}$  are, respectively, the time, electromechanical delay, rising time, decay time and twitch duration. Parameters  $\lambda$ ,  $\lambda_0$  and  $ld$  represent stretch, stretch below which no active tension is generated and the degree of length dependence, respectively.

$T_{peak}$  was set to 200 kPa and 120 kPa for the LV and RV, respectively. The RV was assigned with a smaller tension based on the assumption that the RV has a smaller myocyte density compared to the LV and therefore produces less tension [11]. For both ventricles,  $t_{dur}$  and  $\tau_d$  were set to 450 ms and 100 ms, respectively.

For both atria,  $T_{peak}$  was set to 60 kPa, based on the lower active tension in the atria suggested in the literature [13] with  $t_{dur}$  and  $\tau_d$  set to 200 ms and 50 ms, respectively [8]. The other active stress parameters for both the atria and ventricles were set to:  $t_{emd} = 20.0$  ms,  $\tau_r = 50.0$  ms,  $\lambda = 0.7$  and  $ld = 6.0$ .

## 2.2. Boundary conditions

The effect of the pericardium was simulated with normal springs [4]. A spring stiffness of 10 kPa/mm was scaled in space based on [8]. Additionally, omni-directional springs with spring stiffness of 10 kPa/mm were applied at the superior vena cava and right pulmonary veins. The mechanical contraction was coupled with a closed-loop model for the circulatory system based on CircAdapt [14], [15], with the systemic resistance factor adjusted to achieve a physiological LV pressure. All other parameters were set to the default values [14].

The mesh was generated from an end-diastolic CT image. To achieve an unloaded state, the mesh was iteratively unloaded and reloaded until convergence was reached. The choice of starting point for the simulations is difficult as the state of the tension development in the atria cannot be assumed to be low and homogenous at end-diastole. Therefore, the electromechanics simulation is started at end-diastole but the simulation is run for three heart beats to reduce the effect of this initial condition.

## 3. Results

Figure 2a shows results for the baseline simulations, with full atrial contraction and a HR of 70 bpm. Our model simulated a peak LV pressure of 123 mmHg, which falls within a healthy range [16], and an EF of 42%, which is above the value at which EF is considered to indicate impaired LV function [17]. Figure 2b shows the the geometry of the heart at end-systole compared to end-diastole. The atrioventricular plane moves down during ventricular contraction and there is not significant movement of the apex, consistent with physiological systolic motion.

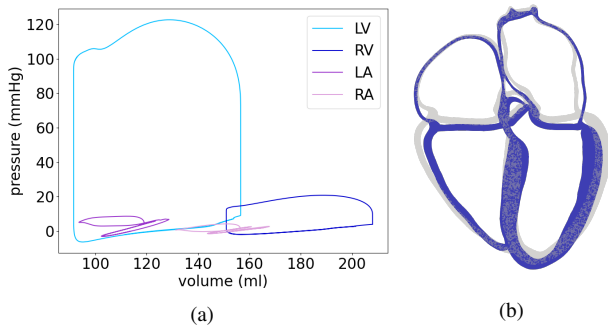


Figure 2: Left: pressure-volume loops for the LV, RV, LA and right atrium (RA). Right: cross-section of the four-chamber model. The grey and blue geometry shows the end-diastolic and end-systolic configurations, respectively.

The effect of HR on LV output was studied by running simulations using two different HRs: 70 bpm and 120 bpm,

representing a normal heart and a typical HR during AF, respectively. The effect of atrial contraction was investigated by turning on and off atrial contraction, setting  $T_{peak}$  for the atria to 0 kPa.

Table 2 and Figure 3 show the results of the simulations. An increased HR and lack of atrial contraction led to a small decrease in EF. However, the interaction between an increased HR and lack of atrial contraction led to a significant drop in EF from 42% to 36%. Furthermore, the maximum pressure in the LV ( $p_{max}$ ) increased with an increase in HR (+20 mmHg) but decreased with a lack of atrial contraction (-3 mmHg). Therefore, in contrast to the effect on EF, the increase in HR and lack of contraction do not act to reinforce one another.

Table 2: Effect of HR and atrial contraction on EF and  $p_{max}$  (mmHg).

Heart rate		Atrial contraction	
		on	off
70	(EF)	42%	41%
	( $p_{max}$ )	123	120
120	(EF)	40%	36%
	( $p_{max}$ )	143	134

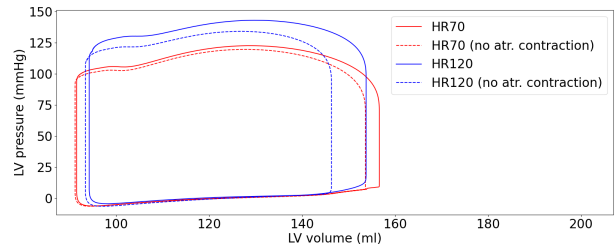


Figure 3: Pressure-volume data from the LV, shown for the last simulated beat.

### 3.1. Limitations

A limitation of this study is that validation of the baseline simulation relies only on achieving physiological values of LV pressure and EF taken from the literature, despite patient-specific data being available. However, fitting the model to patient-specific data would have required a sensitivity analysis which, given the computational expense, was considered to be outside the scope of this work.

A further limitation is that we considered only increased HR and lack of atrial contraction to represent AF. A more advanced study would also consider the effect of irregular HR as this is likely to have a significant effect on left ventricular output.

The use of a phenomenological active tension model is also a limitation of this study, as it does not account for the effect of calcium transient dynamics. This work could be improved by accounting for cross-bridge kinetics and electromechanical coupling through the calcium transient by using a more complex active tension model.

Finally, the simulation predicted a negative pressure at the beginning of diastole in the ventricles and atria, suggesting the pericardium is preventing collapse of the model. This behaviour does not appear to be physiological.

#### 4. Conclusions

Our four-chamber model was able to simulate physiological motion and capture the effects of atrioventricular interaction. This enabled us to show that increased HR and ineffective atrial contraction significantly decrease LV function. These results have implications for further study of AF as they suggest that restoring a normal HR could significantly improve EF, without the need to restore effective atrial contraction. However, investigating the effect of an irregular heart beat will be vital in the future.

#### Acknowledgments

This study received support from the UK Engineering and Physical Sciences Research Council (EP/M012492/1, NS/A000049/1, EP/L015226/1, EP/P01268X/1, EP/P010741 and EP/T517963/1), the Wellcome EP-SRC Centre for Medical Engineering (NS/A000049/1 and WT 203148/Z/16/Z), the British Heart Foundation (PG/15/91/31812 and PG/13/37/30280), the National Institute of Health (NIH R01-HL152256), the European Research Council (ERC PREDICT-HF 864055) and King's Health Partners London National Institute for Health Research (NIHR) Biomedical Research Centre.

#### References

[1] Kornej J, Börschel C, Benjamin E, Schnabel R. Epidemiology of atrial fibrillation in the 21st century. *Circulation Research* Jun. 2020;127(1):4–20.

[2] Stefanadis C, Dernellis J, Toutouzas P. A clinical appraisal of left atrial function. *Eur Heart J* Jan. 2001;2(1):22–36.

[3] Strocchi M, Augustin C, Gsell M, et al. A publicly available virtual cohort of four-chamber heart meshes for cardiac electro-mechanics simulations. *PLoS One* Jun. 2020;15(6).

[4] Strocchi M, Gsell M, Augustin C, et al. Simulating ventricular systolic motion in a four-chamber heart model with spatially varying robin boundary conditions to model the effect of the pericardium. *J Biomech* Mar. 2020;101:109645.

[5] Bayer J, Blake R, Plank G, et al. A novel rule-based algorithm for assigning myocardial fiber orientation to computational heart models. *Ann Biomed Eng* Oct. 2012;40(10):2243–2254.

[6] Rooney C, et al. Variability in pulmonary vein electrophysiology and fibrosis determines arrhythmia susceptibility and dynamics. *PLoS Comput Biol* May 2018;14(5).

[7] Neic A, Campos F, Prassl A, et al. Efficient computation of electrograms and eegs in human whole heart simulations using a reaction-eikonal model. *Journal of Computational Physics* Oct. 2017;346:191–211.

[8] Strocchi M, Augustin C, Gsell M, et al. The Effect of Ventricular Myofibre Orientation on Atrial Dynamics. Cham: Springer International Publishing, 2021.

[9] Guccione J, McCulloch A, Waldman L. Passive material properties of intact ventricular myocardium determined from a cylindrical model. *J Biomech Eng* Feb. 1991;113(1):42–55.

[10] Nasopoulou A, Nordsletten D, Niederer S, Lamata P. Feasibility of the estimation of myocardial stiffness with reduced 2d deformation data. *Lecture Notes in Computer Science* May 2017;10263:357.

[11] Oken D, R.J.Boucek. Quantitation of collagen in human myocardium. *Circulation Research* Jul. 1957;5(4):357–361.

[12] Niederer S, Plank G, Chinchapatnam P, et al. Length-dependent tension in the failing heart and the efficacy of cardiac resynchronization therapy. *Cardiovascular research* Oct. 2010;89:336–43.

[13] Land S, Niederer S. Influence of atrial contraction dynamics on cardiac function. *Int J Numer Method Biomed Eng* Mar. 2018;34(3).

[14] Walmsley J, Arts T, Derval N, et al. Fast simulation of mechanical heterogeneity in the electrically asynchronous heart using the multipatch module. *PLoS* Jul. 2015;11(7).

[15] Augustin C, Gsell M, Karabelas E, et al. Validation of a 3d–0d closed-loop model of the heart and circulation - modeling the experimental assessment of diastolic and systolic ventricular properties. *arXiv Tissues and Organs* 2020;.

[16] Bastos M, Burkhoff D, Maly J, et al. Invasive left ventricle pressure–volume analysis: overview and practical clinical implications. *European Heart Journal* Mar. 2020;41(12):1286–1297.

[17] Zhu K, Ma T, Su Y, et al. Heart failure with mid-range ejection fraction: Every coin has two sides. *Frontiers in Cardiovascular Medicine* 2021;8.

Address for correspondence:

Rosie Barrows  
Department of Biomedical Engineering and Imaging Sciences,  
4th Floor, North Wing, St Thomas' Hospital, London, SE1 7EH  
rosie.barrows@kcl.ac.uk